

## Relation of decay time constants between postseismic deformation and aftershocks of the 2011 Tohoku-Oki earthquake

\*Mikio Tobita<sup>1</sup>

1.Geospatial Information Authority of Japan

Since the 2011 off the Pacific coast of Tohoku Earthquake (Tohoku-Oki earthquake), crustal deformation and aftershocks have continued to occur in eastern Japan. This paper discusses the comparison of their relaxation time constants.

### 1. Introduction

Tobita(2014, 2015, 2016) proposed combined logarithmic (log) and exponential (exp) function model for fitting postseismic GNSS time series after 2011 Tohoku-Oki earthquake. They are log+exp (Model-1), log+log+exp (Model-2) and log+exp+exp (Model-3). The Model-2 has the best performance for the short-term prediction of the evolution of postseismic deformation. The equation that represents the Model-2 is

$$D(t) = a\ln(1+t/b) + c + d\ln(1+t/e) - f\exp(-t/g) + Vt,$$

where  $D(t)$  denotes a displacement component (east, north, or up),  $t$  is the time in days relative to the occurrence of the main shock (11 March 2011),  $b$ ,  $e$  and  $g$  denote the timescale parameters of the logarithmic or exponential decays (relaxation times), and  $V$  is the steady velocity.

We believe that comparison of relaxation time parameters between cumulative number of aftershocks and the postseismic deformation may contribute to discriminate the subsurface postseismic deformation mechanisms.

As the first step, we began to study function fitting of aftershocks by Omori's formula, Modified Omori's formula and ETAS model, then attempt to adopt single exp and single log functions.

### 2. Methods and Results

The bold curve in Fig. 1 represents the cumulative number of aftershocks larger than M5 in the rectangle shown in the map in Fig. 1.

- (1) A single exponential function cannot fit the curve at all.
- (2) Fitting performance by a single logarithmic function is not satisfactory.
- (3) We found that a logarithmic function with background seismicity fits the cumulative aftershocks curve very well.
- (4) The first log term in the equation with relaxation time constants  $b=0.03$  days (preliminary estimate) with the background seismicity ( $\mu$  in Fig. 1) was fitted to the curve of the cumulative number of aftershocks.
- (5) The second log term in the equation with relaxation time constants  $e=49.6$  days (preliminary estimate) with the background seismicity was fitted to the curve.
- (6) The third exp term in the equation with relaxation time constants  $g=4610$  days (preliminary estimate) with the background seismicity was fitted to the curve.

The results of the three fittings (4)-(6) are shown in Fig. 1. While, the second term (log) with mid-term relaxation time (5) and the third term (exp) with long-term relaxation time (6) do not fit the curve at all, the first term (log) with short-term relaxation time (4) fit the curve quite well.

### 3. Discussion

We found that the relaxation time constants of the cumulative number of aftershocks are very similar to that of the first term (log) with short-term relaxation time of postseismic deformation time-series. Tobita (2016) suggests that the short-term log function may represent postseismic displacements due to mainly the afterslip, while the mid-tem log and long-term exp functions may

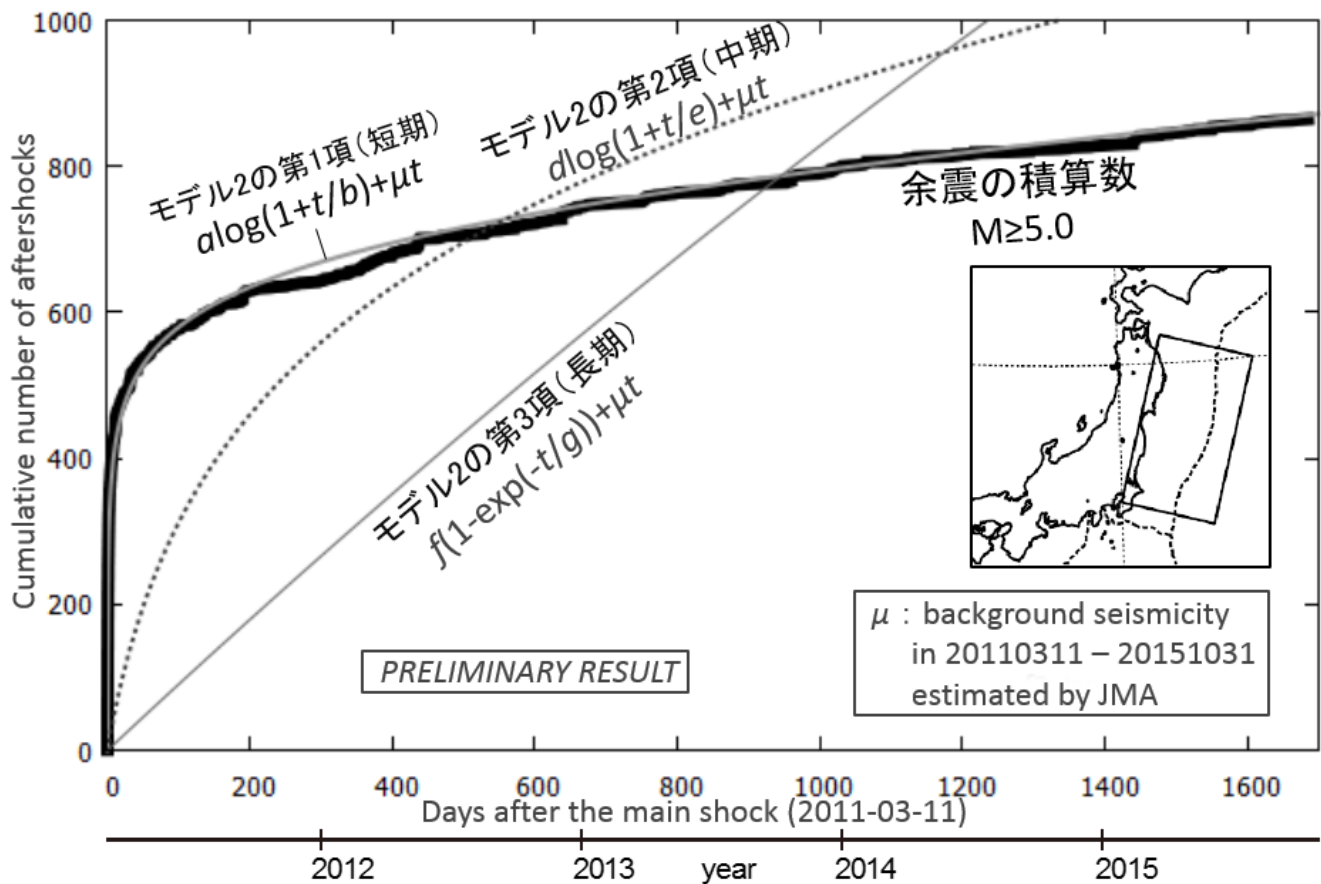
represent postseismic displacements due to mainly the viscoelastic relaxation. Our finding is consistent with the suggestion.

Good fits of the cumulative aftershocks curve by a single log function (with background seismicity) means validity of the Omori's law in the Tohoku-Oki earthquake, because the time integral of the Omori's formula is a logarithmic function.

Acknowledgement

The rectangle in Tohoku area, seismic data, and model parameters of the seismic data were provided by JMA. We appreciate it.

Keywords: 2011 Tohoku-Oki earthquake, postseismic deformation, function fitting, aftershock, viscoelastic relaxation, decay time



## Time series modeling of the postseismic deformation after the 2011 Tohoku earthquake

\*Shunsuke Miura<sup>1</sup>, Mako Ohzono<sup>2</sup>

1. Department of Earth and Environmental Sciences Graduate School, Yamagata University, 2. Faculty of Science, Yamagata University

Time series of the postseismic deformation is often explained by superposition of the logarithmic and exponential time evolutions, which assumes the afterslip and the viscoelastic relaxation, respectively. For the 2011 Tohoku-oki earthquake (M9.0), eastern side of GNSS network is well explained by superposition of those functions (e.g., Tobita, 2015). Miura and Ohzono (2015) also explained postseismic time evolution using F3 daily solution at the 93 GEONET sites in wide region of Tohoku for four years after the earthquake. The estimated time constants of the horizontal component of afterslip and viscoelastic relaxation are ~7 days and ~2500 days, respectively. The vertical displacement has large signal of viscoelastic relaxation along the east coast of the study area. Focusing on spatial distribution of the estimated each signal for four years, we compare our result with other postseismic models. Our result of afterslip estimation shows large horizontal displacement of 100cm at Yamada in eastern part of Iwate. Around this site, from Kwai2 to Rifu in fore-arc relatively large displacements (< 80 cm). This pattern roughly agrees with other result of afterslip modeling (e.g., Silverii *et al.*, 2014; Yamagiwa *et al.*, 2014). On the other hand, some sites that have clear signal are not explained by the previous studies. The vertical displacement pattern, which shows obvious trend in the time series, may be cannot explained by the model. Although the maximum signal of the viscoelastic relaxation is smaller than that of the afterslip, it distributes more extensive region including back-arc side. This uniform displacement pattern will be mostly explained by simple viscoelastic model.

Keywords: postseismic deformation, tohoku earthquake

## Heterogeneous surface deformation of the Kanto plain after the 2011 Tohoku earthquake

\*Kazuya Ishitsuka<sup>1</sup>, Takuya Nishimura<sup>2</sup>, Toshifumi Matsuoka<sup>3,1</sup>

1.Fukada Geological Institution, 2.Disaster Prevention Research Institute, Kyoto University,  
3.Center for the Promotion of Interdisciplinary Education and Research, Kyoto University

Surface deformation of Japan island after the 2011 Tohoku earthquake has been modeled by visco-elastic relaxation and after slip. On the other hand, there were local post-seismic deformation at the Kanto plain that cannot be explained by the common model. In this study, we investigated surface deformation of the Kanto plain from March 2011 to December 2013 using GEONET data and PS-InSAR analysis of TerraSAR-X data. It has been reported that the Kanto region has uplifted after the 2011 earthquake, and the uplift velocity has been faster along with the distance from the epicenter. In addition to the global uplift pattern, we found the uplift velocity was locally faster about several mm/year around the north of Kanagawa Prefecture and the west of Tokyo. The local uplift occurred soon after the earthquake and decayed over about two years. As far as we know, sudden artificial changes such as groundwater usage were not reported in the period, accordingly this local uplift has likely occurred spontaneously. Moreover, our PS-InSAR analysis estimated the uplift occurred with the spatial dimension of about 10-20 km<sup>2</sup>. This study of local post-seismic deformation may reveal local stress perturbation and a post-seismic deformation mechanism that has not been previously concerned.

Keywords: The 2011 Tohoku earthquake, The Kanto plain, Crustal deformation, GEONET, PS-InSAR analysis

## Aseismic slips synchronized with earthquakes in northern Chiba Prefecture, Japan

\*Akio Kobayashi<sup>1</sup>, Fuyuki Hirose<sup>1</sup>

1.Meteorological Research Institute, Japan Meteorological Agency

Episodes of intermittent uplift over periods of one month to a year have been observed by the Global Navigation Satellite System in the northeastern part of Chiba Prefecture, Kanto district, Japan. Uplift in the vicinity of Choshi in 2000 was accompanied by the earthquake near Choshi in June 2000 (M6.1). Uplift of the northeastern part of Chiba Prefecture in 2005 was accompanied by the earthquakes near Choshi in April 2005 (M6.1) and near Chiba-city in July 2005 (M6.0). Although our estimates of the source parameters for these uplifts were well explained by slips on the faults of these earthquakes, the amounts of slip we estimated for the uplifts were several times larger than we expected from the earthquakes. We attribute the extra slip to the above mentioned intermittent uplift events, which we suggest were caused by aseismic slips.

Keywords: Aseismic slip, Northern Chiba Prefecture, GNSS

## Time dependent block fault modeling of southeast Japan

\*Shinzaburo Ozawa<sup>1</sup>

### 1.GSI of Japan

#### Abstract

We conducted time dependent block fault modeling for southeast Japan. The result shows that slip deficit on the Philippine sea plate which takes block motion into account becomes smaller than that which does not take into account block motion. In particular, slip deficit of the Philippine Sea plate in the Tokai inland area disappears, as was confirmed in previous studies by many researchers.

#### Introduction

It is very important to estimated interplate coupling precisely so that we can get information about whereabouts and moment magnitude of the expected large subduction earthquakes. In particular, it is an urgent task to prepare for the Tokai and Tonakai earthquakes along the Suruga and Nankai troughs. Under this circumstance, many studies have been conducted about the interplate coupling in southeast Japan. However, spatial and temporal interplate coupling has not been treated in detail. In this study, we developed an analytical code of time dependent block fault modeling and applied it to southeast Japan.

#### Analytical Procedure

Hashimoto et al(2000) conducted block fault modeling of Japan, using GPS data. In this study, we used the block model geometry of Hashimoto et al. (2000). That is we used rectangular faults in inland area defined by Hashimoto et al. (2000). The plate boundary in a subdcution area was represented by superposition of spline functions. By using this geometry, we estimated interplate coupling in inland area and subduction zones. We used EW, NS, UD position time series at approximately 500 GSP sites. The period was set at 2008-2009

#### Results and Discussion

Time dependent block fault modeling shows that interplate coupling on the Philippine Sea plate decreases when we take into account a block motion. In Tokai region, coupling on the Philippine Sea plate disappears in deep inland area.

Keywords: time dependent inversion, block fault modeling , southeast Japan

## Abnormal strain distribution in Hokkaido, Japan, inferred from the 2003 Tokachi-oki earthquake (M8.0)

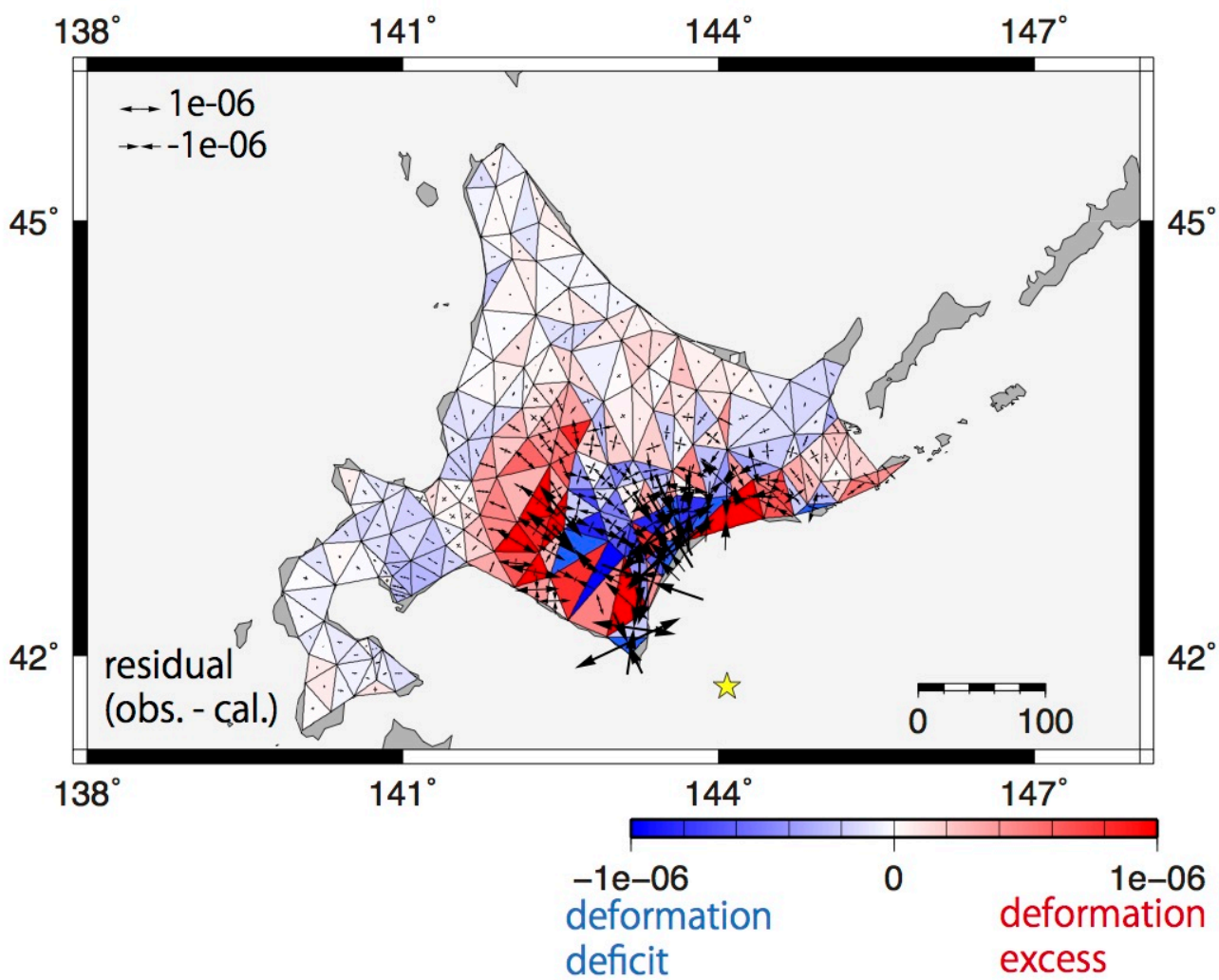
\*Kentaro Ishimori<sup>1</sup>, Mako Ohzono<sup>2</sup>

1.Department of Earth and Environmental Sciences Graduate School, Yamagata University, 2.Faculty of Science, Yamagata University

From the coseismic strain distribution of the 2003 Tokachi-oki earthquake (M8.0) and 2011 Tohoku-oki earthquake (M9.0), we try to examine how big abnormal coseismic strain can correlate to heterogeneous subsurface structure in Hokkaido, Japan. For the 2003 Tokachi-oki earthquake, Ishimori and Ohzono (2015, JpGU) compared coseismic crustal deformation observed from GEONET F3 solutions with theoretical crustal deformation which calculated from dislocation model (Okada, 1992) with a rectangular fault. The result shows  $10^{-7}$  of strain anomaly (difference between observations and calculations), and good agreement of spatial distribution of the strain anomaly region and characteristic subsurface structure, such as thick sedimentary area. This feature is supported by a simulation that suggests the relatively small elastic moduli of the thick sedimentary layer in the upper crust (Yabe et al., 2015). We also estimate the coseismic strain anomaly in Hokkaido at the 2011 Tohoku-oki earthquake. As a result, we found  $10^{-8}$  of coseismic strain anomaly. However, the relationship between the strain anomaly distribution and subsurface structure was not clear. We conclude that that the tiny strain anomaly ( $<10^{-7}$ ) cannot detect characteristic subsurface structure.

For the coseismic strain anomaly of the 2003 Tokachi-oki earthquake, the vectors of principal maximum strain calculated from residual displacements (observations - calculations) indicates relatively large NW-SE convergence axes in eastern part of Hokkaido (Kushiro-Nemuro region). On the other hand, middle size of interplate earthquake, such as 2004 Kushiro-oki earthquake (M7.1) is occurred after the Tokachi-oki earthquake (2003, 1952). Because residual convergence direction agrees with the plate convergence direction, there is a possibility that those earthquakes might be triggered by the large coseismic strain anomaly.

Keywords: 2003 Tokachi-oki earthquake, subsurface structure, abnormal strain





## Coseismic and Postseismic Deformation Related to The 2012 Indian Ocean Earthquake using Three-Dimensional FEM

\*Cecep Pratama<sup>1</sup>, Takeo Ito<sup>1,2</sup>, Fumiaki Kimata<sup>3</sup>, Takao Tabei<sup>4</sup>

1.Graduate School of Environmental Studies, Nagoya University, 2.Earthquake and Volcano Research Center, 3.Tono Research Institute of Earthquake Science, 4.Department of Applied Science, Faculty of Science, Kochi University

On April 11, 2012, a Mw 8.6 earthquake struck off the west coast of northern Sumatra approximately 100 km west of the Sunda trench. The 2012 Indian Ocean earthquake, which is the largest intraplate earthquake in recorded history, yields a total seismic moment of  $13.6 \times 10^{28}$  dyne cm. Aceh GPS Network for Sumatran Fault System (AGNeSS) observed a predominantly ENE coseismic offset of up to 10 cm while the sites on the Andaman Island and southern part of Sumatra GPS Array (SuGaR) network observed southward and northward, respectively. In order to construct more realistic surface displacement due to complex subduction region, we consider developing inhomogeneous three-dimensional finite element model incorporate subducting slab, three-dimensional velocity earth structure, realistic topography and bathymetry. We infer uniform slip for six fault planes using fault geometry as reported from Hill et al. (2015). In the other hand, the time series of continuous GPS site coordinates clearly exhibit postseismic displacements. We parameterized the displacements time series due to previous earthquakes and remove pre-earthquake trend from the time series. The corrected time series of permanent GPS data shows that the relaxation time in the vertical component displacement is longer than horizontal component displacements. This discrepancy indicates multiple physical mechanisms. We proposed a mechanical model, which refer to afterslip and viscoelastic relaxation, to explain postseismic deformation following to the 2012 Indian Ocean Earthquake.

Keywords: Coseismic, Postseismic, GPS, FEM

## Investigating the crustal deformation on the Hazar-Palu segment of the East Anatolian Fault (EAF), Turkey

\*WUMITI JULAITI<sup>1</sup>, Semih Ergintav<sup>1</sup>, Ziyadin Cakir<sup>2</sup>, Ugur Dogan<sup>3</sup>, Selver Senturk<sup>2</sup>, Seda Cetin<sup>3</sup>, Hayrullah Karabulut<sup>1</sup>, Fuat Saroglu, Haluk Ozener<sup>1</sup>

1.Bogazici University, 2.Istanbul Technical University, 3.Yildiz Technical University

As well known, strike-slip faults are a fault type widely spread around the world. Many of them are located at boundaries between two tectonic plates. For instance, the East Anatolian Fault (EAF), the one in this study, forms a 400-km-long boundary between the Anatolian and the Arabian plates. It is a typical left-lateral slip fault with an ENE-WSW strike and a total offset of 33 km. As it is easy to obtain velocity solution from GPS raw data on a specific block or plate with the software, here is GAMIT/GLOBK, one can estimate the long-term slip rate as well as creeping zone, locking depth and the offset between two nearly-rigid blocks of a fault or between the fault's surface trace and the dislocation below the seismogenic zone by using inter-seismic GPS velocities and proper models. However, not many suchlike studies have been carried out along the whole EAF as those done on North Anatolian Fault (NAF) during the last 20 years. Most of them are focused on the area around the triple junction where the Dead Sea Fault connects to the EAF and the overall deformation using mainly InSAR. Moreover, there are only a few large earthquakes documented since the last century and InSAR based studies indicate that low seismicity can be related with a creep mechanism that may reach to 10 mm/yr creep rate, along different segments of the EAF. Based on the recent published GPS velocities, the slip rate on EAF is estimated about 8 to 10 mm/yr, which seems that the strain accumulation will not occur and therefore the creeping zone of EAF will not produce a remarkable earthquake. But the extent of the creeping zone is not well constrained, which still implies the potential of the seismic hazard arising.

The aim of this study here is to perform the velocity solutions from the present-day cGPS sites' data (Turkey's National Permanent GPS Network-ACTIVE data, i.e. TUSAGA-ACTIVE data) and new sGPS observations (up-to-date surveys based on proper profiles) on particular segment of EAF, the Hazar-Palu segment, which may be combined with the more recent InSAR observations, to develop an appropriate inter-seismic deformation model around this region with a multidisciplinary perspective.

Keywords: creep, GPS, East Anatolian Fault, slip rate

## Computation of uplift rate caused by present-day ice melting in Southeast Alaska

\*Kazuhiro Naganawa<sup>1</sup>, Takahito Kazama<sup>1</sup>, Yoichi Fukuda<sup>1</sup>

1. Graduate School of Science, Kyoto University

Crustal uplift caused by ice melting is observed in glacial areas such as Antarctica, Greenland and Alaska. This uplift consists of elastic and viscoelastic effects, which are called post glacial rebound (PGR) and present-day ice melting (PDIM), respectively. By dividing these effects from observed geodetic data, geophysical parameters such as mantle viscosity can be estimated.

In Southeast Alaska, for example, many geodesists have studied spatiotemporal characteristics of the crustal uplift due to ice melting. Sun et al. (2010) collected absolute gravity values in Southeast Alaska once a year from 2006 to 2008, and calculated the rate of the uplift due to PDIM ( $d\Delta/dt$ ) from the absolute gravity and GPS data. They also estimated the  $d\Delta/dt$  values by the spatial integral of a PDIM model, showing the spatial distribution of the ice melting rate around Southeast Alaska. However, the amplitudes of the  $d\Delta/dt$  values were not consistent with each other, possibly because Sun et al. (2010) simplified the conditions of their model calculation, especially about the distance between glaciers and each gravity site.

We were thus motivated to accurately estimate the rate of the PDIM-derived uplift at six absolute gravity sites in Southeast Alaska using PDIM models and observed geodetic data ( $d\Delta/dt(\text{obs})$  and  $d\Delta/dt(\text{cal})$ , respectively). We first calculated  $d\Delta/dt(\text{cal})$  by the spatial integral of the UAF07 PDIM model (Larsen et al., 2007) using a response function of crustal deformation to a disk load (Farrell, 1972). We also calculated  $d\Delta/dt(\text{obs})$  from the rates of the GPS uplift and absolute gravity change from 2006 to 2013 (Kazama et al., 2015) using equations based on Wahr et al. (1995).

The average value of  $d\Delta/dt(\text{obs})$  at six gravity sites was calculated to be  $14.7 \pm 2.2$  mm/year, and its standard deviation is smaller than that of Sun et al. (2010) ( $10.7 \pm 7.3$  mm/year) because we utilized the precise values of the gravity variation rates by Kazama et al. (2015), who considered the absolute gravity data newly obtained in 2012 and 2013. In addition, the average value of  $d\Delta/dt(\text{cal})$  was estimated to be  $10.3 \pm 1.4$  mm/year, which corresponded to 70 % of  $d\Delta/dt(\text{obs})$  in this study. Our  $d\Delta/dt(\text{cal})$  value reproduced the  $d\Delta/dt(\text{obs})$  value more than that of Sun et al. (2010) ( $5.5 \pm 3.2$  mm/year; 50 % of their  $d\Delta/dt(\text{obs})$  value), because we considered realistic distributions of glaciers and gravity sites in estimating  $d\Delta/dt(\text{cal})$  from the PDIM model. The  $d\Delta/dt(\text{cal})$  value in this study still differs with  $d\Delta/dt(\text{obs})$  by about 30 %, which implies that more realistic conditions should be considered in the model calculation, such as the curvature, topography or internal structure of the Earth, and/or updated PDIM models.

Keywords: load deformation, ice sheet melting, gravity change, crustal uplift, Alaska

## Spatial variation in Earth structure inferred by GNSS seasonal deformations due to snow loads

Rie Kurisu<sup>2</sup>, \*Hitoshi Hirose<sup>1</sup>, Takuya Nishimura<sup>3</sup>

1.Research Center for Urban Safety and Security, Kobe University, 2.Graduate School of Science, Kobe University, 3.Disaster Prevention Research Institute, Kyoto University

Seasonal variations are observed in GNSS site coordinate time series (e.g., Murakami and Miyazaki, 2001; Munekane et al., 2004). Heki (2001) showed that snow loads cause seasonal subsidence in winter in the Tohoku region, northeast Japan from the Geospatial Information Authority of Japan's (GSI) GEONET GNSS daily site coordinates during the period 1999.0-2001.0. It becomes worth reevaluating this issue because the observed GNSS data are accumulated over 10 years and the amplitude of apparent seasonal components can be reduced with revised analysis strategies (e.g., Nakagawa et al., 2009). Here we show that the correlation between a seasonal variation and snow depth over 10 years is good in some areas with the largest snow depths among the study areas, the ratio of seasonal subsidence to snow depth shows spatial variation, and the variation can be explained by spatial variation of underground structure.

We obtain daily coordinate time series at GEONET sites in the Tohoku region by applying GIPSY-OASIS II software (version 6.3) (Zumberge et al., 1997) to observed phase data provided by GSI. A seasonal signal in vertical component for each year is estimated for each site. These seasonal signals are compared with daily snow depth measurements at AMeDAS sites. We use data at 135 GEONET sites and 102 AMeDAS sites in the Tohoku region during the period 1999.5-2009.5.

The Tohoku region is divided into a number of areas as large as 0.5 degree in latitude and 0.5 degree in longitude in order to find spatial variation in the correlation between the seasonal signal and the snow depth. We calculate an averaged seasonal signal for each area from the seasonal signals of individual GEONET sites in the area. Similarly, an averaged snow depths are calculated for each area. These averages are converted to time series of monthly values. We find a correlation coefficient larger than 0.6 on most areas with the maximum averaged snow depth > 150 cm. We estimate the ratio of seasonal subsidence to snow depth (defined as "the ratio b") from the monthly values on these areas. The ratio b of the range 0.021-0.053 mm/cm is obtained from five areas among eight areas where maximum snow depths are higher than 150 cm (three areas are eliminated because subsidence due to pumping of groundwater in winter is suggested).

For comparison with the observed ratio b, we compute the expected ratio b assuming the Gutenberg-Bullen A Earth model (Sato et al., 1968) with snow density of the range 0.2-0.5 g/cm<sup>3</sup> (Kawashima et al., 2007) using SPOTL (Agnew, 1996). In this case, the ratio b of the range 0.0083-0.021 mm/cm (defined as "b<sub>basement</sub>") is expected. b<sub>basement</sub> is smaller than the observed ratio b, indicating that the observed subsidence is larger than the calculated one assuming a global Earth model without a softer sediment layer.

Next we estimate the ratio b for a sedimentary basin because the study area includes Niigata basin where one of the thickest sediment layer is observed in Japan. Assuming averaged values of V<sub>p</sub>, V<sub>s</sub>, and for the Niigata sediment layer (Koketsu, 2008), Young's modulus of 7.2 GPa, and then the strain of 2.7-6.8e-7 are obtained under the same snow load as b<sub>basement</sub>. Assuming that deformation caused by snow load occurs in the sedimentary layer with the thickness of 8 km (J-SHIS, <http://www.j-shis.bosai.go.jp>), subsidence of 2.2-5.4 mm and the ratio b (b<sub>sediment</sub>) of 0.022-0.054 mm/cm is expected. Although this estimation is very rough, the ratio b<sub>sediment</sub> can explain the observed ratio b, which is larger than b<sub>basement</sub>. Therefore, the spatial variation of the ratio b observed by GNSS can not be explained by the variation in snow density only, and an

additional amplifying factor, possibly an effect of softer sedimentary layer, must be required. This study shows a possibility to be able to probe the spatial variation of the elastic response to snow loads with GNSS.

Keywords: Deformation by surface load, Seasonal variation in crustal deformation, Sedimentary layer

## Theoretical calculation of internal stress/strain changes caused by earthquakes: the effectiveness of the reciprocity theorem in a spherical earth

\*Yu Takagi<sup>1</sup>, Shuhei Okubo<sup>2</sup>

1.School of Science, The University of Tokyo, 2.Earthquake Research Institute, The University of Tokyo

Co-seismic deformation (e.g. stress and strain changes) within the Earth has been estimated by using Okada's (1992) formulae for a semi-infinite homogeneous medium. An example is seen in estimation of Coulomb's static stress changes. However, when stress or strain changes caused by great earthquakes are estimated, we should use a more realistic earth model including the effects of Earth's curvature and layered structure; the stress changes caused by the 2011 Tohoku-oki earthquake exceed 0.1 bar even at the epicentral distance over 400 km (Toda et al., 2011). In principle, Takeuchi & Saito (1972) showed a recipe to calculate deformations due to earthquakes in a spherical earth model. In practice, however, there are some computational problems in order to realize the computation of internal deformations. One of them is loss of significant digits (LSD). We found that a method using the reciprocity theorem (Okubo, 1993) can avoid this problem. In this presentation, we will show that the conventional method cannot avoid the LSD whereas the method using reciprocity theorem can.

After Takeuchi & Saito (1972), the equations governing co-seismic deformation field result in first-order inhomogeneous differential equations by expanding displacement and stress by the spherical harmonics. To solve these differential equations, in the conventional method, (i) we obtain the complementary solutions, (ii) find the particular solution, and (iii) add them so that the final solution satisfies the surface boundary condition. The magnitude of the final solution is the order of  $(r_s/r_p)^n$ , where the  $r_s$  and  $r_p$  ( $>r_s$ ) are the radii where the source is located and the deformation is evaluated, respectively, and  $n$  is the degree of the spherical harmonics. On the other hand, the magnitude of the solutions obtained by the process (i) and (ii) is the order of  $(r_p/r_s)^n$ . This means that, in process (iii), LSD cannot be avoided at a large degree  $n$  because we need to add the numbers whose magnitude is  $(r_p/r_s)^n/(r_s/r_p)^n=(r_p/r_s)^{2n}$  times larger than that of the final solution. For example, the ratio  $(r_p/r_s)^{2n}$  becomes  $10^{12}$  at  $n=8,000$  when the deformation at a depth of 10 km ( $r_p=6361$  km) due to a source at a depth of 20 km ( $r_s=6351$  km) is considered. We confirmed that LSD occurs around  $n=8,000$  in actual computation.

In the method using the reciprocity theorem, we obtain (a) the solutions  $x_1$  at the radius  $r_s$  caused by external sources such as tide and (b) a solution  $x_2$  that has a unit jump at the radius  $r_p$ . They are easily calculated by numerical integration. (c) Finally, the final solution is obtained by multiplying  $x_1$  and  $x_2$  together. This means that we can avoid the LSD that occurs in doing addition.

Keywords: co-seismic deformation, internal deformation, spherically symmetric earth, reciprocity theorem

A change of the crustal vertical ground deformation estimated from the repetition observation of a leveling

\*Kazutomo Takano<sup>1</sup>

1.GSI of Japan

The Geospatial Information Authority of Japan (GSI) is carrying out the repetition observation of a leveling in the Tokai region from Morimachi to Omaezaki. In the present study, I conducted the examination from the observation of the leveling about the anomalous vertical ground deformation considered to have generated in this region around 2000 to 2005.

Keywords: leveling, crustal vertical deformation, Tokai region

## Vertical Deformation Detected by the Precise Levelling Survey in the Periods of Before and After the 2014 Mt. Ontake Eruption and Their Interpretations (2006-2015)

\*Masayuki Murase<sup>1</sup>, Fumiaki Kimata<sup>2</sup>, Yoshiko Yamanaka<sup>3</sup>, Shinichiro Horikawa<sup>3</sup>, Kenjiro Matsuhira<sup>3</sup>, Takeshi Matsushima<sup>4</sup>, Hitoshi, Y. Mori<sup>5</sup>, Shin Yoshikawa<sup>6</sup>, Rikio Miyajima<sup>2</sup>, Hiroyuki Inoue<sup>6</sup>, Kazunari Uchida<sup>4</sup>, Keigo Yamamoto<sup>7</sup>, Takahiro Ohkura<sup>6</sup>, Manami Nakamoto<sup>4</sup>, Masahiro Yoshimoto<sup>3</sup>, Takashi OKUDA<sup>3</sup>, Taketoshi Mishima<sup>6</sup>, Tadaomi Sonoda<sup>7</sup>, Shintaro Komatsu<sup>7</sup>, Kaito Katano<sup>1</sup>, Keiji Ikeda<sup>8</sup>, Hiroaki Yanagisawa<sup>8</sup>, Shigeru Watanabe<sup>8</sup>, Haruhisa Nakamichi<sup>7</sup>

1.Department of Earth and Environmental Sciences, College of Humanities and Sciences, NIHON University, 2.Tono Research Institute of Earthquake Science, Association for the Development of Earthquake Prediction, 3.Research Center for Seismology Volcanology and Disaster Mitigation, Graduate School of Environmental Studies, Nagoya University, 4.Institute of Seismology and Volcanology, Faculty of Sciences, Kyushu University, 5.Institute of Seismology and Volcanology, Graduate School of Science, Hokkaido University, 6.Aso Volcanological Laboratory, Graduate School of Science, Kyoto University, 7.Sakurajima Volcano Research Center, Disaster Prevention Research Institute, Kyoto University, 8.Japan Meteorological Agency

We conducted the precise leveling survey in Ontake volcano in April 2015 and discussed vertical deformations detected in the Periods of Before and After the 2014 Mt. Ontake Eruption (2006-2015). Notable uplift (2006-2009) and subsidence (2009-2014) were detected on the eastern flank of the volcano. We estimated pressure source models based on the vertical deformation and used these to infer preparatory process preceding the 2014 eruption. Our results suggest that the subsidence experienced between 2009 and 2014 (including the period of the 2014 eruption) occurred as a result of a sill-like tensile crack with a depth of 2.5 km. This tensile crack might inflate prior to the eruption and deflate during the 2014 activity. A two-tensile-crack model was used to explain uplift from 2006 to 2009. The geometry of the shallow crack was assumed to be the same as the sill-like tensile crack. The deep crack was estimated to be 2 km in length, 4.5 km in width, and 3 km in depth. Distinct uplifts began on the volcano flanks in 2006 and were followed by seismic activities and a small phreatic eruption in 2007. From the partially surveyed leveling data in August 2013, uplift might continue until August 2013 without seismic activity in the summit area. Based on the uplift from 2006 to 2013, magma ascended rapidly beneath the summit area in December 2006, and deep and shallow tensile cracks were expanded between 2006 and 2013. The presence of expanded cracks between 2007 and 2013 has not been inferred by previous studies. A phreatic eruption occurred on 27 September 2014, and, following this activity, the shallow crack may have deflated. In the period between October 2014 and April 2015, small uplift less than 4mm was detected.

Keywords: Ontake volcano, precise leveling survey, deformation



Opening crack associated with the 2015 eruption of the Hakone volcano estimated from InSAR

\*Ryosuke Doke<sup>1</sup>, Masatake Harada<sup>1</sup>, Ryou Honda<sup>1</sup>, Yohei Yukutake<sup>1</sup>, Kazutaka Mannen<sup>1</sup>, Jun Takenaka<sup>1</sup>

1.Hot Springs Research Institute of Kanagawa Prefecture

Seismic activities on the Hakone Volcano, which located western part of Kanagawa Prefecture, Japan, were activated from the end of April, 2015. Then, small phreatic eruptions occurred at the Owakudani from 29th June. From the InSAR analysis by using ALOS-2/PALSAR-2 data, we detected a crustal deformation which caused by an opening crack formed during the eruption. Based on the inversion modeling of InSAR data, we defined the geometric and kinematic characteristics of the opening crack.

Estimated crack is trending NW-SE direction and dipping 82.2°NE, with 1.3 km in length and 0.3 km in width. Opening displacement was estimated to be 14.5 cm in a rectangular model. The opening distribution was estimated through the linear inversion, under the condition that the position and orientation of crack were fixed. The result showed that two peaks of opening were in the central shallow part and southern part. Volume changes of the crack were estimated  $5.6 \times 10^4 \text{ m}^3$  in the rectangular model and  $6.6 \times 10^4 \text{ m}^3$  in the linear model. It is considered that the intrusion of hot water or steam to the crack excited the swelling and triggered the eruption at Owakudani.

Keywords: Hakone Volcano, 2015 phreatic eruption, InSAR, Opening crack, Modeling

## Rainfall correction of the Extensometer at Matsushiro

\*Kazuhiro Kimura<sup>1</sup>, Akio Kobayashi<sup>1</sup>, Minoru Funakoshi<sup>2</sup>

1.Meteorological Research Institute, 2.Matsushiro Seismological Observatory, Earthquake and Tsunami Observation Division, Seismological and Volcanological Department, Japan Meteorological Agency

Japan Meteorological Agency (JMA) installed the quartz tube extensometer of 100m in the tunnel at Matsushiro (Nagano city, Japan). This extensometer data is stable for several decades, but is influenced by the rainfall. Nishimae and Wakui (1996) tried the rainfall correction using a tank model for N-S component of this extensometer. They successfully estimated parameters of the model by trial and error.

We estimate parameters of the tank model by Shuffled Complex Evolution method developed at the University of Arizona (SCE-UA method). The parameters estimated are similar each other. In addition, we introduce the rainfall correction by the tank model of E-W component of this extensometer.

Keywords: Extensometer, rainfall correction, shuffled complex evolution method developed at the university of arizona

## Morphometric evaluation of tectonic activity in the northern Ochigata fault zone in the Southern Noto Peninsula, north-central Japan

\*Hiroyuki Yamaguchi<sup>1</sup>, Akira Takeuchi<sup>2</sup>

1. Graduate School of Science and Engineering for Education, University of Toyama, 2. Graduate School of Science and Engineering for Research, University of Toyama

The Ochigata fault zone consists of a 44 km long active faults in a NE-SW direction, from the northern edge to the western part of the Hodatsu hill in the neck of Noto Peninsula, Ishikawa Prefecture. The fault zone is divided into five segments from north to south: the Sekidosan fault, the Furuko fault, the Nodera fault, the Tsuboyama-Hachino fault and the fault of near Uchitakamatsu. The Sekidosan, the northern Nodera and the Uchitakamatsu faults are reverse in slip sense dipping to the east. The southern Nodera and the Tsuboyama-Hachino fault are reverse faults dipping to the west. Their latest event and recurrence interval are revealed by trench investigations performed at the central Sekidosan fault, and pointed out that the uplifting was finished before the Middle Pleistocene based of the geologic structure. However, the pattern of tectonic activity through the fault zone is unclear.

This study examined tectonic deformation of the northern Ochigata fault zone using Mountain-front sinuosity ( $S_{mf}$ ) and the ratio of valley floor width to valley height ( $V_f$ ), which were morphometric indices for representing tectonic activity.  $S_{mf}$  is explained as the ratio of length of mountain front along the foot of mountain to the straight length of mountain front. The poorer development of sinuosity means the higher uplift rates, and is consistent with the lower value of  $S_{mf}$ .  $V_f$  is explained by the ratio of width of valley floor to relative elevation between ridge and valley floor. In an area with high uplift rates, topographic profile illustrates a V-shaped profile with the both lower values. This study calculated the value of  $V_f$  at a position of 200 m on the mountain side from mountain front. In our morphometric analysis, the 5m-DEM of the Geospatial Information Authority of Japan publication was utilized, and was combined with the slope map and the over ground openness map for interpreting geomorphology of the mountain front.

Separating the mountain front of Sekidosan fault into 22 sections and the northern Nodera fault into 3 sections, the values of  $S_{mf}$  within the Sekidosan fault ranged from 3 to 6 at the northern part, 2 to 3.5 at the central and 4 to 25 at the southern. The values of  $S_{mf}$  at the northern Nodera fault were 3.5 to 11. The values of  $V_f$  within the Sekidosan fault were 2 to 6 at the northern part, 0.5 to 3 at the central and 4 to 35 at the southern. The values of  $V_f$  at the northern Nodera fault ranged from 4 to 6. The both indices for the Sekidosan fault performed lower at the center part, and the values of the northern and southern parts of Sekidosan fault and those of the northern Nodera fault became higher. In other words, tectonic activity of the northern Ochigata fault zone is the highest at the central Sekidosan fault and the activity tend to decrease towards the both terminations of Sekidosan fault and the northern Nodera fault.

No case study on  $S_{mf}$  and  $V_f$  has ever been done in Japan. To examine the quantitative relationship between the two indices and uplift rates, it is important to accumulate the more geological and geomorphological data.

Keywords: morphometric analysis, tectonic activity, Ochigata fault zone